**Structural Engineering and Mechanics**, *Vol. 69, No. 1 (2019) 95-104*
DOI: https://doi.org/10.12989/sem.2019.69.1.095


# Evaluation of ASCE 61-14 NSPs for the estimation of seismic demands in marginal wharves

J. Paul. Smith-Pardo*[1], Juan C. Reyes[2a], Juan D. Sandoval[2b] and Wael M. Hassan[3c]

[1]*Department of Civil and Environmental Engineering, Seattle University, Seattle, USA*
[2]*Department of Civil and Environmental Engineering, Universidad de los Andes, Bogotá, Colombia*
[3]*Department of Civil Engineering, University of Alaska, Anchorage, USA*

*(Received June 6, 2018, Revised November 22, 2018, Accepted November 23, 2018)*

**Abstract.** The Standard ASCE 61-14 proposes the Substitute Structure Method (SSM) as a Nonlinear Static Procedure (NSP) to estimate nonlinear displacement demands at the center of mass of piers or wharves under seismic actions. To account for bidirectional earthquake excitation according to the Standard, results from independent pushover analyses in each orthogonal direction should be combined using either a 100/30 directional approach or a procedure referred to as the Dynamic Magnification Factor, DMF. The main purpose of this paper is to present an evaluation of these NSPs in relation to four wharf model structures on soil conditions ranging from soft to medium dense clay. Results from nonlinear static analyses were compared against benchmark values of relevant Engineering Design Parameters, EDPs. The latter are defined as the geometric mean demands that are obtained from nonlinear dynamic analyses using a set of 30 two-component ground motion records. It was found that SSM provides close estimates of the benchmark displacement demands at the center of mass of the wharf structures. Furthermore, for the most critical pile connection at a landside corner of the wharf the 100/30 and DMF approaches produced displacement, curvature, and force demands that were reasonably comparable to corresponding benchmark values.

**Keywords:** pushover analysis; nonlinear static procedure (NSP); ASCE 61 standard; marginal wharves; performance-based design

## 1. Introduction

Ports are essential to the world economy and in places like the United States they are used to handle goods amounting to over 10% of the gross domestic product, GDP (Port of Seattle, 2013). In New Zealand, ports transfer up to 99% of all exports and imports by volume, thus making them important to the financial success of the region (Ragued *et al.* 2014). Unfortunately, the combination of earthquakes with soft soil conditions in coastal zones often render port infrastructure susceptible detrimental consequences. Downtime associated to earthquake damage can compromise operations of port facilities and cost even more than actual repairs. Following the Hyogo-Ken Nanbu earthquake, for example, damage to the Port of Kobe was estimated to be U.S. $11 billion (Landers 2001) and six years later the facility had only recovered 80% of its trade while competitors in the area increased their container-handling volume by twofold. The importance of port infrastructure to emergency response was highlighted with the 2010 Haiti Earthquake after extensive damage to two wharves in Port-au-Prince and one wharf in Carrefur limited the delivery of international aid and crippled rescue activities (Eberhard *et al.* 2010). Damage and partial collapse of the structures were attributed to catastrophic failures of the sand fills which included liquefaction, lateral spreading, and differential settlements (DesRoches *et al.* 2011). Interestingly, a post-earthquake site investigation of the wharf in Port-au-Prince revealed that the overall response of the artificial fill was consistent with predictions from semi-empirical relations (Green *et al.* 2011).

Many of the busiest ports in the world are in regions of moderate and high seismic risk. Considering their relevance, it is necessary for designers to develop a deeper understanding of their performance under major earthquakes. Contributing to that effort Varun *et al.* (2013) presented a macro-element model for soil-structure interaction analyses of piles in liquefiable soils. The model accounted for soil resistance and radiation damping with increasing material nonlinearity and was successfully validated using full-scale forced vibration and centrifuge tests. Chore *et al.* (2012) studied the lateral load behavior of pile groups modeled with beam elements supported on soil springs (py-curves). It was found that consideration of non-linearity of the soil can increase the lateral displacement at the pile top by as much as 150%. Similarly, Saha *et al.* (2015) demonstrated that shear demands on piles depend largely on their relative stiffness with respect to the superstructure and the supporting soil. At a system level,

*Corresponding author, Associate Professor
E-mail: smithjh@seattleu.edu
[a]Associate Professor
E-mail: jureyes@uniandes.edu.co
[b]Graduate Research Assistant
E-mail: jd.sandoval3153@uniandes.edu.co
[c]Associate Professor of Structural and Earthquake Eng.
E-mail: wmhassan@alaska.edu



ISSN: 1225-4568 (Print), 1598-6217 (Online)

multiple studies have been published on the seismic analysis of marginal wharves under strong ground motions. Roth and Dawson (2003), for example, conducted FLAC analyses of three pile-supported wharves in the Port of Oakland, California, which suffered various degrees of structural damage under the 1989 Loma Prieta earthquake. Wharf piles were represented with elasto-plastic beam elements connected to a grid of nonlinear soil springs and the resulting model was useful to reproduce some of the damage that was observed in the field. Shafieezadeh *et al.* (2012) evaluated the vulnerability of pile-supported marginal wharves in the West Coast of the United States which were designed decades using seismic design provisions that are now obsolete. Using advanced structural and soil modeling techniques in response history analyses, they found that under large seismic events wharf structures can experience large permanent deformations and failures of pile-deck connections including pullout of batter piles. More recently, Shafieezadeh *et al.* (2013) presented the results of a detailed three-dimensional nonlinear response of a pile-supported wharf in liquefiable soils. It was found that the oscillating component of embankment deformations was the primary contributor to the demands on piles and their connections to the deck, while the effects of permanent deformation of the embankment soil were less significant. These analyses showed the importance of modeling the three-dimensional characteristics of the system to properly capture the coupled longitudinal and torsional response of the structure, especially for impulsive near field motions.

In collaboration with the New Zealand port authorities, Ragued *et al.* (2014) defined generic wharf configurations representative of local geotechnical characteristics and typical structural details including tie-back wharves and wharves with one pair of batter piles per bent. They developed fragility curves that allow estimating the probability of a structure/component reaching a defined damage state or engineering design parameter (EDP) value for a given peak ground acceleration. For low intensity ground motions, no significant difference in the performance of wharves with different configurations was obtained. However, for high intensity the seismic performance of tie-back wharves was significantly better than that of marginal wharves with one batter pile per bent. This finding is consistent with earthquake reconnaissance reports highlighting the vulnerability of batter piles during strong earthquakes (Zareian *et al.* 2012). Recently, Shafieezadeh *et al.* (2014) developed a resilience assessment of a hypothetical seaport under moderate to severe seismic events. The latter could serve as framework that enables stakeholders assess the most likely performance of a port system under future earthquakes. Similarly, Burden *et al.* (2016) developed a methodology to estimate earthquake-induced losses of pile-supported wharves including repair costs and downtime. Results were expressed in the form of loss exceedance curves for seismic risk management of port infrastructure.

Seismic design guidelines and regulations for pile-supported piers and wharves have not evolved at the same speed as those for buildings or bridges. Historically, the design of waterfront structures has relied only on guidelines such as California Building Standards (2010) and POLA (2012). As a result, wharf/pier designers often needed to extrapolate provisions that were developed for other types of structures. In response to the need for standardization and as a first step toward regulating the seismic design of waterfront structures in the United States, the Coast Ocean Ports and Rivers Institute (COPRI) created a committee in 2005 to produce a standard document that reflects the state of practice in the design of piers and wharves supported on piles. Recognizing also recent developments of earthquake engineering, standard ASCE/COPRI 61-14 (2014), referred to as ASCE 61 hereafter, was first released. Acceptable methods in this standard to analyze wharves under seismic actions are nonlinear static procedures (NSPs) and nonlinear dynamic analyses. In the first case, EDPs-such as displacements, forces, material strains-may be estimated using the results from pushover analyses. With the second procedure, EDPs are directly calculated via nonlinear response history analyses (RHAs) of a computer model subjected to a suite of ground motion records. It is well known that the nonlinear RHA provides more accurate estimates of EDPs, however, the computational demand may be prohibitive in terms of time or budget constraints so practitioners opt to use pushover procedures more often.

The objective of the study is to evaluate the nonlinear static procedures (NSPs) available in ASCE 61, for the seismic analysis of marginal wharves under bi-directional excitation. It is important to emphasize that the main intent of this research is not to support the standard but to assess the accuracy of its pushover procedure as applied to wharf structures. The evaluation is conducted using four case studies that are representative of current design practice of container terminals and include soil conditions ranging from soft to moderately dense. The implemented assessment methodology is the same as that used by other researchers to test pushover or ground motion scaling procedures [Baker and Cornell (2006), Kalkan and Chopra (2010), Kalkan and Chopra (2012), Reyes and Chopra (2011a), Reyes and Chopra (2011b), Reyes and Chopra (2012), Reyes and Quintero (2013), Reyes *et al.* (2014) and Reyes *et al.* (2015)). The latter involves using the results of nonlinear RHAs as benchmarks for evaluation.

## 2. ASCE 61-14 nonlinear static procedures (NSPs) and EDPs

For facilities of high design classification (essential to a region's economy or post-earthquake recovery), the standard ASCE 61 requires that the seismic performance of pier or wharf structures be evaluated under two hazard levels: a) Operational Level Earthquake (OLE), which represents an event with a 50% probability of exceedance in 50 years; and b) Contingency Level Earthquake (CLE), which corresponds to an event with a 10% probability of exceedance in 50 years. The structure must be designed for minor damage under OLE and repairable damage under CLE. In addition, the wharf or pier must be designed to meet a life safety performance level under a design level earthquake (DE) such that from traditional building codes. Acceptance performance criteria to assess damage under

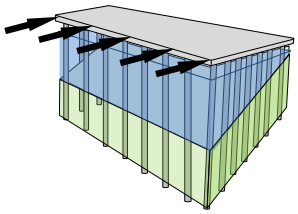

(a) Transverse direction

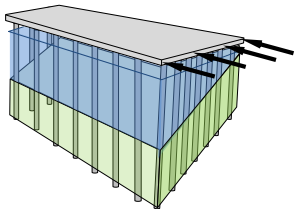

(b) Longitudinal direction

Fig. 1 Wharf pushover analysis

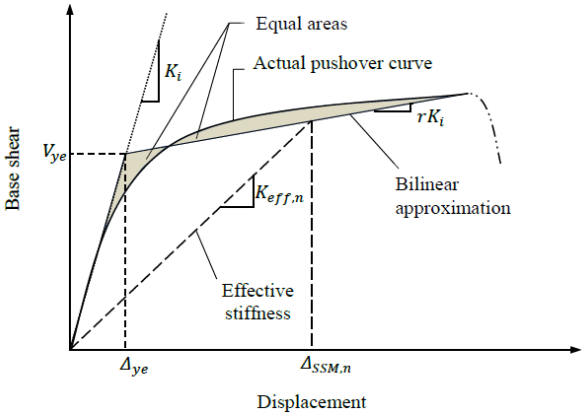


Fig. 2 Idealized pushover curve (adopted from ASCE 61)

each of these hazard levels are given in terms of material strain limits for piles and their connections. Superstructure components, on the other hand, must be detailed using capacity-protection design principles to guarantee that they remain nearly undamaged under any seismic hazard level.

The nonlinear static procedures (NSPs) included in ASCE 61 require the execution of lateral load (pushover) analyses of the structure and use of the Substitute Structure Method (SSM) to estimate the displacement demand at the center of mass-also known as target displacement. Once displacements have been determined, two alternatives may be used for estimating Engineering Design Parameters (EDPs) under bi-directional ground excitation: a) orthogonal combination (100/30), and b) dynamic modification factor (DMF). A description of these procedures is presented in the following.

### *2.1 Substitute structure method (SSM)*

The substitute structure method was originally developed by Shibata and Sozen (1976) and is based on the premise that the maximum response of an inelastic system can be satisfactorily simulated by an equivalent linear system with reduced lateral stiffness and increased equivalent viscous damping. Although Chopra and Goel (2001) have demonstrated that displacement-based design procedures using elastic design spectra for equivalent linear systems may underestimate displacement and ductility demands, their analyses were limited to single-degree-of-freedom systems or building structures that could be represented by a single mode. The latter is not the case for marginal wharf structures where the presence of piles with radically different lateral stiffness (from the waterside to the landside) can lead to significant torsional effects. The steps to implement the SSM in the analysis of marginal wharves, as implied in ASCE 61 standard, are as follows:

Step1) Calculate the base shear-versus-center of mass displacement relation (pushover curve) of the structure subjected to a uniform lateral load pattern in either the transverse or longitudinal direction of the wharf or pier (Fig. 1).

Step 2) Find a bilinear base shear-versus-displacement such as the area under the approximate relation up to the peak lateral load is equal to the area under the actual pushover curve (Fig. 2). Determine the initial stiffness $K_i$, and the ratio $r$ between the slopes of the two lines defining the bilinear approximation.

Step 3) Assume a trial target displacement $\Delta_{SSM,n}$ demand at the center of mass of the wharf for a given design pseudo-acceleration spectrum.

Step 4) Use the bilinear approximation of the pushover response to calculate an effective lateral stiffness $K_{eff,n}$ of the structure for the trial target displacement (Fig. 2)

$$K_{eff,n} = \frac{V_n}{\Delta_{SSM,n}} \tag{1}$$

Step 5) Calculate the effective fundamental period of the structure $T_n$ as an equivalent single-degree-of-freedom system

$$T_n = 2\pi\sqrt{\frac{m}{K_{eff,n}}} \tag{2}$$

where $m$ is the effective mass of the wharf; which includes the superstructure, attached fixtures, and 10% of the design live load.

Step 6) Read a trial acceleration value $S_{a,n}$ from the design pseudo-acceleration spectrum for a period $T_n$ and 5% damping ratio. If the period of the structure in the given direction of analysis is less than the period corresponding to the peak spectral acceleration, then a revised design pseudo-acceleration spectrum should be calculated using an effective damping ratio given by

$$\zeta_{eff,n} = 0.05 + \frac{1}{\pi}\left(1 - \frac{1-r}{\sqrt{\mu_n}} - r\sqrt{\mu_n}\right) \tag{3}$$

where $\mu_n = \Delta_{SSM,n}/\Delta_{ye}$ is the trial displacement ductility demand, and $\Delta_{ye}$ is the yielding displacement corresponding to the intersection of the two linear segments in the idealized bilinear approximation of the pushover curve (Fig. 2).

$$\Delta_{SSM,n} = S_{a,n}\frac{T_n^2}{4\pi^2} \tag{4}$$

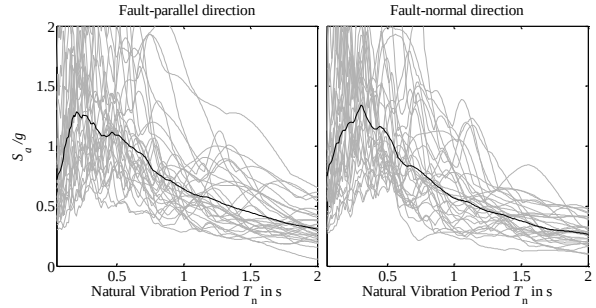


Fig. 3 Response spectra (light lines) for selected 30 ground motion records and geometric mean (design) spectrum (dark line) for five percent damping ratio

Step 7) Calculate a new trial target displacement

Step 8) Repeat steps 3 to 7 until the difference between the new and the previous trial target displacements is less than 3%. Denote the latest trial as the target displacement, $\Delta_{SSM}$.

Step 9) Repeat steps 1 to 8 to determine $\Delta_{SSM}$ due to excitation in the other orthogonal direction of the structure (longitudinal or transverse).

### *2.2 Alternatives in ASCE 61 for estimating Engineering Design Parameters (EDPs)*

The nonlinear target displacements that are obtained with the SSM can be used in conjunction with one of the two procedures described below to estimate EDPs for wharf structures under bidirectional ground excitation.

a) 100/30 directional combination:

This refers to the traditional approach that is used in building codes to estimate demands due to simultaneous ground motion excitation in the transverse and longitudinal direction of the structure. Design values of EDPs may be estimated using Eq. (5)

$$E = max\begin{cases}\pm 0.3E_t \pm 1.0E_l \\ \pm 1.0E_t \pm 0.3E_l\end{cases} \quad (5)$$

where, $E_t$ and $E_l$ are the EDPs corresponding to target displacement in the transverse and longitudinal direction of the wharf, respectively, while $E$ is the resultant EDP.

In order to calculate $E_t$, the structural model must be subjected to a uniform lateral load pattern in the transverse direction only (Fig. 1(a)), until the displacement of the center of mass equals the transverse target displacement that was obtained using the substitute structure method, $(\Delta_{SSM})_t$. Similarly, $E_l$ is obtained by subjecting the model of the structure to a uniform lateral load pattern in the longitudinal direction (Fig. 1(b)) until the center of mass reaches the target longitudinal displacement, $(\Delta_{SSM})_l$.

b) Dynamic magnification factor (DMF):

In this procedure, which was originally developed by Benzoni and Priestley (2003) for wharf structure segments (supported on octagonal piles) with length to width aspect ratio greater than three, the total displacement demand of the wharf $\Delta_d$ is related to displacement demand in the transverse direction $\Delta_t$ through the expression

Table 1 Ground motion records used in this study

| ID | Earthquake Name | Year | Station Name | $M_w$ | $R_{closest}$ (km) | Site Class |
|---|---|---|---|---|---|---|
| 1 | Imperial Valley-06 | 1979 | El Centro Array No 8 | 6.5 | 3.9 | D |
| 2 | Imperial Valley-06 | 1979 | El Centro Differential Array | 6.5 | 5.1 | D |
| 3 | Imperial Valley-06 | 1979 | EC County Center FF | 6.5 | 7.3 | D |
| 4 | Imperial Valley-06 | 1979 | El Centro Array No 10 | 6.5 | 8.6 | D |
| 5 | Superstition Hills-02 | 1987 | Poe Road (temp) | 6.5 | 11.2 | D |
| 6 | Corinth Greece | 1981 | Corinth ss | 6.6 | 10.3 | C |
| 7 | Northridge-01 | 1994 | Pacoima Kagel Canyon | 6.7 | 7.3 | C |
| 8 | Northridge-01 | 1994 | Sun Valley - Roscoe Blvd | 6.7 | 10.1 | D |
| 9 | Northridge-01 | 1994 | Canyon Country-W Lost Canyon | 6.7 | 12.4 | D |
| 10 | Nahanni Canada | 1985 | Site 2 | 6.8 | 4.9 | C |
| 11 | Nahanni Canada | 1985 | Site 1 | 6.8 | 9.6 | C |
| 12 | Chuetsu-oki Japan | 2007 | Kawanishi Izumozaki | 6.8 | 11.8 | D |
| 13 | Gazli USSR | 1976 | Karakyr | 6.8 | 5.5 | D |
| 14 | Kobe Japan | 1995 | Nishi-Akashi | 6.9 | 7.1 | C |
| 15 | Loma Prieta | 1989 | Corralitos | 6.9 | 3.9 | C |
| 16 | Loma Prieta | 1989 | Saratoga - Aloha Ave | 6.9 | 8.5 | C |
| 17 | Loma Prieta | 1989 | Saratoga - W Valley Coll. | 6.9 | 9.3 | D |
| 18 | Loma Prieta | 1989 | Gilroy Array No 3 | 6.9 | 12.8 | D |
| 19 | Imperial Valley-02 | 1940 | El Centro Array No 9 | 7.0 | 6.1 | D |
| 20 | Cape Mendocino | 1992 | Cape Mendocino | 7.0 | 8.0 | C |
| 21 | Cape Mendocino | 1992 | Bunker Hill FAA | 7.0 | 12.2 | C |
| 22 | Montenegro | 1979 | Ulcinj - Hotel Albatros | 7.1 | 4.4 | C |
| 23 | Montenegro | 1979 | Ulcinj - Hotel Olimpic | 7.1 | 5.8 | D |
| 24 | Montenegro | 1979 | Bar-Skupstina Opstine | 7.1 | 7.0 | C |
| 25 | Hector Mine | 1999 | Hector | 7.1 | 11.7 | C |
| 26 | Duzce-Turkey | 1999 | IRIGM 498 | 7.1 | 3.6 | C |
| 27 | Duzce-Turkey | 1999 | Duzce | 7.1 | 6.6 | D |
| 28 | Duzce-Turkey | 1999 | Bolu | 7.1 | 12.0 | D |
| 29 | Landers | 1992 | Joshua Tree | 7.3 | 11.0 | C |
| 30 | Manjil-Iran | 1990 | Abbar | 7.4 | 12.6 | C |

$$\Delta_d = \Delta_t \sqrt{1 + \left(0.3 + \frac{6e}{L_l}\right)^2} \quad (6)$$

where *e*, or eccentricity, is the transverse distance between the center of mass and the center of rigidity, and $L_l$ is the length of the wharf segment in the longitudinal direction. The second term on the right side of Eq. (6) is called the dynamic magnification factor, DMF.

Although not explicitly stated in ASCE 61, $\Delta_d$ corresponds to the maximum diagonal displacement at the top of the piles located in the inshore corners of the structure; however, to conduct the pushover analysis for wharves with square piles, maximum displacements in the longitudinal and transverse directions are required. In general, information given in the Standard about this procedure is limited and makes its implementation ambiguous. For this reason, the procedure implemented herein is based on the original work by Benzoni and

Priestley (2003) and involves the following steps:

• Calculate the target displacements at the center of mass $(\Delta_{SSM})_l$ and $(\Delta_{SSM})_t$ in the longitudinal and transverse directions, respectively, by using the procedure outlined in Section 2.1.

• Impose to the inshore corner pile, displacements equal to $(\Delta_{SSM})_l$ and $0.30(\Delta_{SSM})_t + 6(\Delta_{SSM})_l e/L_l$ in the longitudinal and transverse directions, respectively; estimate pile EDPs by conducting a nonlinear static analysis.

• Impose to the inshore corner pile, displacements equal to $0.30(\Delta_{SSM})_l$ and $(\Delta_{SSM})_t + 6(0.30\Delta_{SSM})_l e/L_l$ in the longitudinal and transverse directions, respectively; estimate the pile EDPs by conducting a nonlinear static analysis.

• Calculate the maximum EDPs on the inshore corner pile as the maximum of the seismic demands obtained in the previous two steps.

## 3. Ground motion records

Table 1 lists the 30 ground motion records selected for this study. They correspond to near-field earthquakes with moment magnitudes between 6.5 and 7.4, and fault distances ranging from 3.6 to 12.8 km. None of the records was pulse-like so near-fault effects were not expected to have significant effect on the response of the structural models. All the records were amplified by a factor of 1.5 to ensure that the models of the case study structures could be driven well into their inelastic range of response. The pre-amplified records were then resolved into fault-parallel (FP) and fault-normal (FN) components and the corresponding pseudo-acceleration spectra were calculated as shown in Fig. 3 with light gray lines. For implementing the SSM in the calculation of the inelastic transverse and longitudinal displacement demands (target displacements), the geometric mean spectrum of the 30 records -shown with a black thick line- was selected as the design pseudo-acceleration spectrum in each direction.

## 4. Case study structures

### *4.1 Description*

Pile-supported waterfront facilities are long structures often conformed by transverse frames connected through a deck superstructure. In practice, these facilities are denoted as finger pier or marginal wharf depending on whether their longer plan dimension is perpendicular or parallel to the shoreline. Container wharves are commonly designed for high live loads of up 50 kN per square meter, which combined with stringent durability requirements lead to the need for massive superstructures. Piles, on the other hand, are often long to reach competent soil bearing layers while also accommodating the large drafts of modern container vessels. As a result, the condition of strong beam-weak column (pile) is inherent to this type of structure.

A generic plan view and construction sequence of the case study structures is illustrated in Fig. 4 and specific

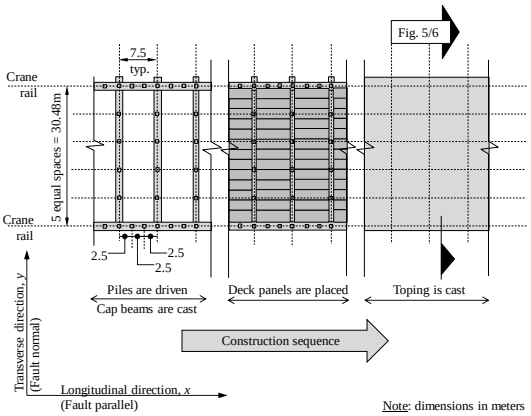


Fig. 4 Wharf structure plan view and construction sequence

cross-sectional views are shown in Figs. 5 and 6. For convenience and to facilitate the discussions, the longitudinal and transverse directions are denoted by the *x*-axis and the *y*-axis respectively. The marginal wharf structures considered in this study were supported by 610 mm (24 in.) square pre-stressed concrete. The first and second structures, henceforth denoted as Wharf 1 and Wharf 2, had 43 transverse bents at 7.5 m on-center spacing. Wharf 3 and Wharf 4, on the other hand, consisted of 85 transverse bents at 7.5 m spacing. The two sets of structures are representative of container terminals with the capability to respectively provide one and two berths for Panamax container vessels. Each wharf had two longitudinal bents at 30.48 m (100 ft) on-center, which support the rails for ship-to-shore (STS) gantry cranes. Pile spacing in those longitudinal bents was 2.5 m to support large crane wheel loads. The longitudinal direction (*x*) of each wharf was assumed to be parallel to the causative fault of the ground motion record, while the fault-normal (FN) component of each ground motion was assumed to be in the transverse direction (*y*) of the structure (Fig. 4). The framing system consisted of piles and transverse pile caps that support 350 mm-thick precast/prestressed concrete panels spanning in the longitudinal direction of the wharf. The panels and the pile caps have sufficient transverse reinforcement projecting into a 200 mm-thick cast-in-place (CIP) concrete topping to ensure composite behavior. Piles were pre-tensioned through 24-12.7 mm (1/2 in.)-diameter grade 270 (1860 MPa) strands and made of concrete with a nominal compressive strength of 42 MPa. Pile-to-deck connection consisted of 16-32 mm diameter (#10) grade 60 (420 MPa) reinforcement. The case study structures were proportioned using ACI 318-14 (2014) for gravity loads and displacement-based provisions in standard ASCE 61 for seismic actions. The latter was based on the geometric mean pseudo-acceleration spectra shown in Fig. 3.

Soil conditions included in this study range from soft to medium dense clay as characterized by the properties listed in Table 2. For simplicity, a single layer of soil was considered in the analyses although the variation of physical properties with depth was also modeled. Mudline slopes were 1:2 and 1:3.5 (vertical to horizontal) in correspondence with the medium dense and soft soils conditions.

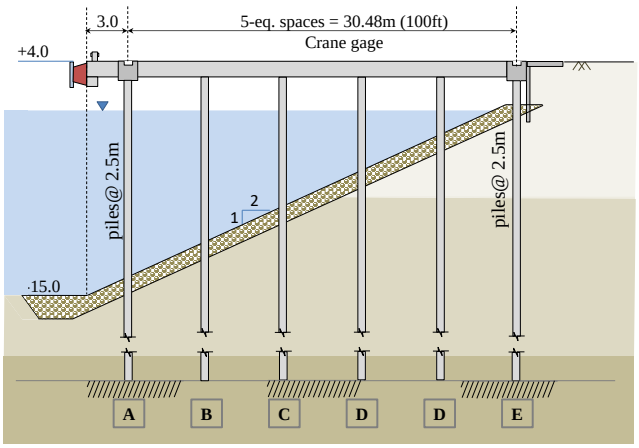


Fig. 5 Cross-sectional view of case study structures on medium dense clay: Wharf 1 (315 m long) and Wharf 3 (630 m long)

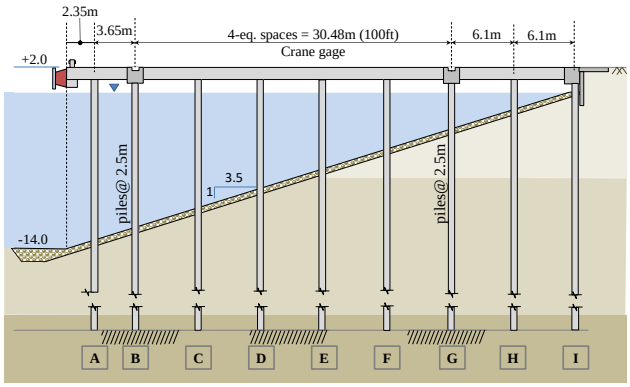


Fig. 6 Cross-sectional view of case study structures on soft clay: Wharf 2 (315 m long) and Wharf 4 (630 m long)

Table 2 Soil properties for case study structures

| Property | Soft soil (1:3.5 slope) | Medium dense soil (1:2 slope) |
|---|---|---|
| Unit weight, kN/m$^3$ | 20 | 20 |
| Cohesion coeff., kN/m$^2$ | 30 | 45 |
| Friction angle, degree | 18 | 22 |
| Soil type | Soft clay | Clay |

### *4.2 Modeling alternatives*

Nonlinear response history analyses (RHAs) of the case-study wharves were conducted using the finite element method software platform PERFORM 3D (Computers and Structures, Inc. 2006). Assuming expected material properties and considering shear deformations in all cases, the following modeling alternatives were explored prior to the execution of dynamic analyses:

• Model alternative 1: Continuum model with soil springs. Nonlinear material fibers were used to represent piles and pile caps, while deck panels were modeled with shell elements. Restraining effect of the soil on the piles was represented using nonlinear lateral springs (also known as py-curves) with force-displacement relations that depend on depth (Matlock 1970).

• Model alternative 2: Macro model with soil springs. Piles and pile caps were modeled as linear elastic elements with plastic hinges at their ends. Cycled strength deterioration and axial load-moment interaction were accounted by using a formulation proposed by El-Tawil and Deierlein (2001a, b). A plastic hinge length of 0.3 m was used in the concentrated plasticity model. Restraining effects of the supporting soil were represented using nonlinear lateral springs.

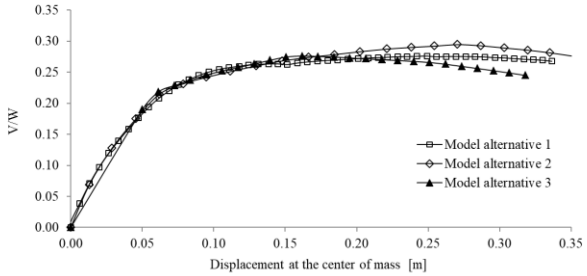


Fig. 7 Pushover response of Wharf 1 in the transverse ($y$) direction for different modeling alternatives

• Model alternative 3: Macro model with fixed-base piles. Pile and pile caps were represented by linear elastic elements with plastic hinges at their ends (El-Tawil and Deierlein, 2001a, b). Plastic hinge length was again equal to 0.3 m. Soil nonlinear springs were not included in the analyses; instead, piles were fixed at a certain depth below mudline. The depth to pile fixity was selected to produce similar force-displacement responses as compared to those from modeling alternatives 1 and 2.

Fig. 7 shows the calculated lateral load response of Wharf 1 in the transverse direction ($y$) for the different modeling alternatives. The horizontal axis corresponds to the displacement at the center of mass at the deck level, while the vertical axis shows the base shear normalized by the seismic weight of the structure. It can be observed that the comparison between the modeling options is favorable. Because using equivalent fixed-base piles reduces the computational demand significantly, this alternative was used for the RHAs and the evaluation of nonlinear static procedures (NSPs) of ASCE 61. It must be noticed that the selection of modeling alternative 3 is conservative as it underestimates the peak shear response and the deformation capacity, while overestimating the strength decay rate at high levels of displacement.

### *4.3 Modal analysis*

Figs. 8 and 9 show the calculated effective modal mass ratios along with schematic representations of the first three mode shapes and corresponding periods of the four case-study structures with fixed-base piles. It is observed that there is strong coupling between the longitudinal displacement ($x$-direction) and plan rotation in the first and third mode, while transverse displacements ($y$) dominate the second mode of vibration. These are consistent with the fact that in the longitudinal direction the structure's center of stiffness is expected to be near the middle of the deck due to symmetry, while in the transverse direction the center of stiffness is close to the shorter (and stiffer) piles on the

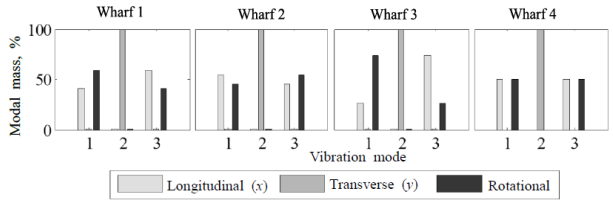


Fig. 8 Effective modal mass for the case study structures

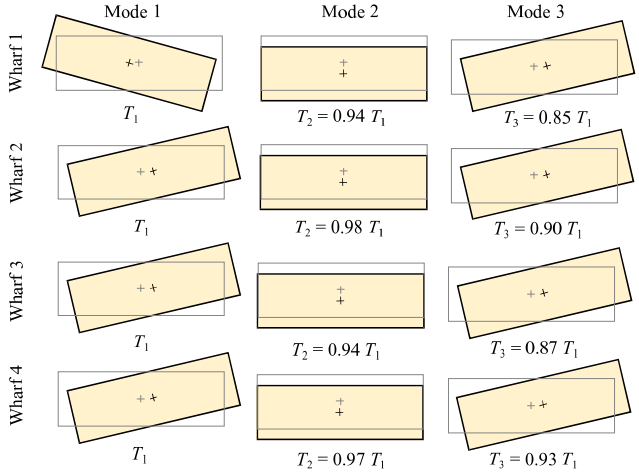


Fig. 9 Schematic views of the calculated first three mode shapes and vibration periods of case study structures

Table 3 Analysis results in the longitudinal direction

| Parameter | Wharf 1 | Wharf 2 | Wharf 3 | Wharf 4 |
|---|---|---|---|---|
| $K_i$, kN/m | 1.08E6 | 1.03E6 | 2.65E6 | 1.95E6 |
| $r$ | 0.076 | 0.193 | 0.058 | 0.281 |
| $T_n$, s | 1.64 | 1.76 | 1.52 | 1.77 |
| e*, m | 13.2 | 13.8 | 13.2 | 13.9 |
| $DMF = \sqrt{1 + (0.3 + 6e/L_l)^2}$ | 1.14 | 1.15 | 1.09 | 1.09 |
| $(\Delta_{SSM})_l$, m | 0.178 | 0.185 | 0.169 | 0.185 |
| $(\Delta_{BENCHMARK})_l$, m | 0.156 | 0.179 | 0.142 | 0.181 |

*transverse distance between center of mass and center of stiffness

Table 4 Analysis results in the transverse direction

| Parameter | Wharf 1 | Wharf 2 | Wharf 3 | Wharf 4 |
|---|---|---|---|---|
| $K_i$, kN/m | 1.01E6 | 1.03E6 | 2.40E6 | 1.95E6 |
| $r$ | 0.174 | 0.279 | 0.143 | 0.281 |
| $T_n$, s | 1.44 | 1.61 | 1.34 | 1.61 |
| $(\Delta_{SSM})_t$, m | 0.136 | 0.146 | 0.128 | 0.146 |
| $(\Delta_{BENCHMARK})_t$, m | 0.138 | 0.160 | 0.140 | 0.161 |

landside and thus significantly offset from the center of mass.

### *4.4 Model dynamic properties and displacement demands at the CM*

Tables 3 and 4 summarize the calculated parameters that characterize the wharf models in the longitudinal and transverse directions. Implementation of the substitute structure method (SSM) in each direction independently led to longitudinal target displacements $(\Delta_{SSM})_l$ that were around 30% greater than the transverse target displacements$(\Delta_{SSM})_t$. The difference is mostly due to the torsional effects on the wharf under longitudinal excitation. It is observed that despite its simplicity, SSM provides reasonable estimates of the benchmark displacement demands in both directions. The method appears conservative with errors of up to 19% for the longitudinal direction of analysis, and unconservative, but with errors of up to 9% only, in the transverse direction of analysis. There is no clear trend regarding the ability of the SSM to produce conservative or unconservative results for the two wharf lengths or the two supporting soil conditions investigated in this study. However, the effective fundamental periods corresponding to the target displacement of the structures on medium dense soils (Wharves 1 and 3) are shorter than those of counterpart structures on soft clay (Wharves 2 and 4), as expected.

## 5. Assessment of ASCE 61 procedures for calculating EDPs

After calculation of target displacements using the SSM, engineering design parameters (EDPs) can be estimated by using a 100/30 orthogonal combination of demands in the two main directions (Section 2.2a) or the DMF approach (Section 2.2b). The inshore corner pile connection was selected to describe the seismic response of the case study structures. Such particular connection is expected to experience the highest demands of any other substructure components of the wharf during an earthquake because: a) wharf torsion affects corner piles the most; b) inshore piles are much stiffer than waterside piles due to the relatively shorter unsupported lengths; c) force demands at the top end of piles are greater than those in the embedded portion since the deck superstructure is stiffer than the supporting soil, and d) pile connections are usually weaker than the piles themselves. Selected EDPs include curvature, displacement, axial load, shear, and moment demands.

Figs. 10 through 13 show calculated EDPs at the critical inshore corner pile connection for the four case-study wharf structures. Calculated values of EDPs for other connections and in-ground hinges of the piles are not included in this paper for conciseness but they can be found in Sandoval (2015). Calculated peak EDPs were normalized by the corresponding benchmark values, which are listed in Table 5. The latter were obtained as the geometric mean of the peak demands from time history analyses with the 30 two-component ground motion records of Section 3. In all cases, the dispersion from RHAs is shown with a shaded region bounded by the 25$^{th}$ and the 75$^{th}$ percentile of the calculated EDPs, which are also normalized by the corresponding benchmark values.

It can be observed from Table 5 that, as expected, displacement demands for the structures on relative stiff soil (Wharves 1 and 3) are smaller than the displacement demands on the counterpart structures on soft soils (Wharves 2 and 4). It is seen that there is very little

Table 5 Benchmark values for EDP of inshore corner pile connection

| EDP | Wharf 1 | Wharf 2 | Wharf 3 | Wharf 4 |
|---|---|---|---|---|
| Curvature around $x$-axis$_1$ (1/m) | 0.038 | 0.048 | 0.041 | 0.048 |
| Curvature around $y$-axis$_2$ (1/m) | 0.038 | 0.049 | 0.041 | 0.045 |
| Displacement in $x$-dir$_1$ (m) | 0.157 | 0.176 | 0.141 | 0.180 |
| Displacement in $y$-dir (m) | 0.153 | 0.165 | 0.148 | 0.167 |
| Axial load (kN) | 1310 | 1210 | 1340 | 1180 |
| Moment around $x$-axis$_1$ (kN-m) | 1640 | 1720 | 1670 | 1700 |
| Moment around $y$-axis$_2$ (kN-m) | 1470 | 1740 | 1580 | 1700 |
| Shear in $x$-dir$_1$ (kN) | 372 | 419 | 419 | 371 |
| Shear in $y$-dir$_2$ (kN) | 374 | 407 | 421 | 353 |

$_1x$-axis coincides with longitudinal direction of the wharf (also fault-parallel direction).
$_2y$-axis coincides with transverse direction of the wharf (also fault-normal direction)

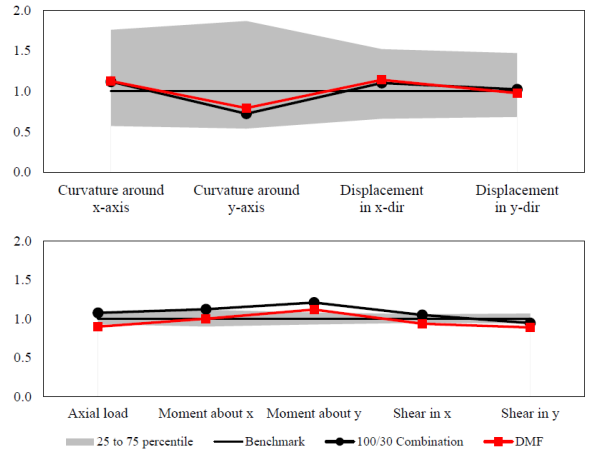


Fig. 10 Normalized EDPs for critical pile connection of Wharf 1

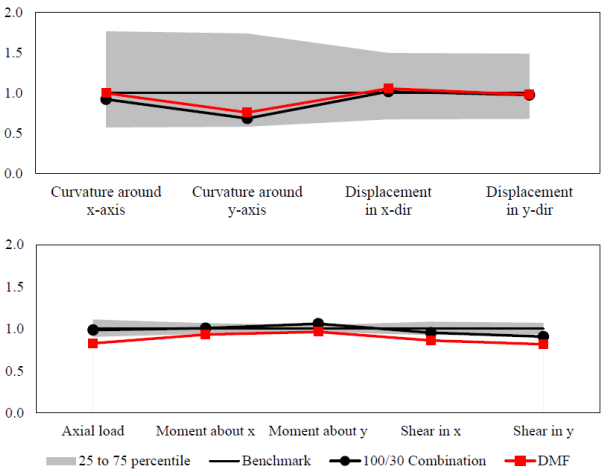


Fig. 11 Normalized EDPs for critical pile connection of Wharf 2

difference in the peak displacement demands on the critical inshore corner pile for a one-berth structure versus the two-berth structures on soft soil (Wharves 2 and 4). Table 5 also shows that the curvature and moment demands are higher for the structures on softer soil (Wharves 2 and 4) as compared to the counterpart structures on stiff soil (Wharves 1 and 3). The change in wharf geometry for a stiff versus a soft soil can help explain this counterintuitive result. The wharf on the soft soil is wider and the short piles (on the land side) have more tributary superstructure inertial forces as compared to the narrower wharf on stiffer soil. In addition, the distance between the center of mass and center of stiffness is also bigger for the wharf on soft soil and thus torsional effects are more significant in thse critical landside corner piles as compared to those for the wharf on stiff soil.

Several observations and conclusions can be drawn from Figs. 10 through 13, that are important to emphasize:

• The two directional combination procedures evaluated in this study - 100/30 orthogonal combination and DMF- are consistent with each other as they provide similar estimates of both force EDPs (moment, shear, and axial load) and deformation EDPs (displacement and curvature).

• The amount of dispersion in the calculated force demands is very small. This is because for all ground motions included in this study, the level of excitation was significant to drive the corner inshore pile well into its nonlinear range of response. Because these piles hinge at the connection with the platform and in-ground (as represented by the point of fixity), peak shear and moment demands are similar from one record to the next.

• The estimation of forces from using either 100/30 directional combination or the DMF approach are within 20% of the benchmark values. However, in some cases the results from these two methods fall outside the first to third quartile values obtained from nonlinear dynamic analyses. Fortunately, for a displacement-based design-which is the preferred approach in the standard ASCE 61- the exact estimation of force demands is not critical.

• The dispersion in the estimated curvature and displacement demand is significantly more than that of force demands. The 100/30 orthogonal combination and the DMF approaches, however, produce estimates of displacements and curvatures that are well within the amount of scatter from nonlinear dynamic analyses. As a result, the two procedures are deemed adequate for the displacement-design of marginal wharves such as those included in this study.

• The 100/30 orthogonal combination and the DMF approach both produce very good estimates of the curvature demands about the $x$-axis (longitudinal direction) as compared to benchmark values. The methods give conservative estimates by 10 to 20% for structures on stiff soils (Wharves 1 & 3) and nearly identical estimates for structures on soft soils (Wharves 2 & 4).

• For all four case study structures considered in this study, the 100/30 orthogonal combination and the DMF approach produce underestimations of the curvature demand with respect to the $y$-axis with errors as high as 30%. This means that the NSPs in ASCE 61 are less accurate for longitudinal ground motions (producing curvature demands with respect to the transverse $y$-axis mostly) than for transverse ground motions (producing curvature demands with respect to the x-axis). This is

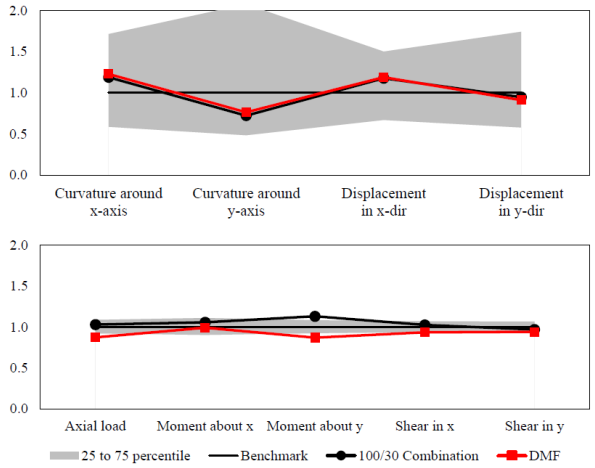


Fig. 12 Normalized EDPs for critical pile connection of Wharf 3

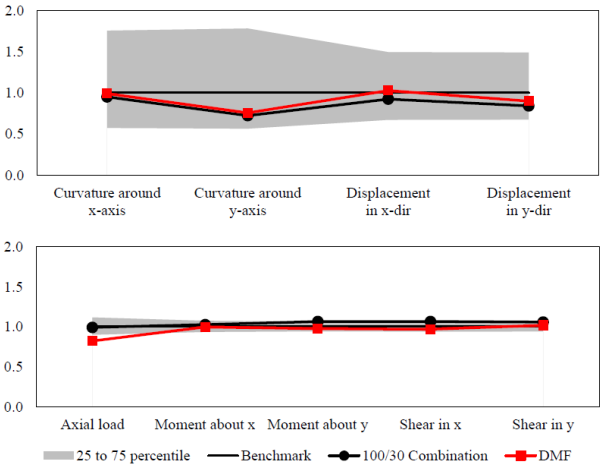


Fig. 13 Normalized EDPs for critical pile connection of Wharf 4

related to the fact that transverse excitation of the wharf triggers a single mode while the longitudinal excitation affects two modes, including torsion.

## 6. Conclusions

Nonlinear static analysis procedures available in the standard ASCE61-14 were used to estimate critical Engineering Design Parameters (EDPs) for four wharf structure models-representative of a range of conditions of practical interest. The evaluation was performed in relation to the geometric mean of peak values obtained from nonlinear dynamic analyses of models under two-component ground motions. A total of 30 earthquake records defining a plausible seismic scenario without near fault effects were used to conduct the time history analyses. Wharf structures were modeled using different levels of refinement, including material fiber models coupled with nonlinear soil springs and concentrated plasticity (plastic hinge) models that account for the interaction between moment, axial load, and curvature. The use of a concentrated plasticity model and pile point of fixity was adequate to reproduce the nonlinear lateral force-versus-displacement response of more elaborate finite element models.

Using the geometric mean of 30 records as the design pseudo-acceleration spectrum in each direction independently, the substitute structure method (SSM) was found to provide reasonable estimates of the displacement demands at the center of mass of the structures, as compared to the geometric mean values from RHAs of the same ground motions, regardless of the length of the wharf or supporting soil conditions. The SSM was conservative for excitations in the longitudinal direction and slightly unconservative for excitations in the transverse direction of the structure. It was also found that using SSM in conjunction with either the 100/30 directional combination or the dynamic magnification factor (DMF) approaches provided reasonably consistent EDP estimates for the inshore corner pile-to-superstructure connection. Moment, shear, and axial load estimates at that critical connection were within 20% of corresponding benchmark values; whereas displacements and curvature demands were within the 25 to 75 percentile values obtained from nonlinear dynamic analyses. It is concluded therefore that using the ASCE 61 nonlinear static procedures to calculate EDPs is appropriate for the seismic design of wharf structures such as those included in this study.

## References

ACI 318 (2014), *Building Code Requirements for Structural Concrete*, American Concrete Institute, Farmington Hills.

ASCE/COPRI 61-14 (2014), *Seismic Design of Piers and Wharves,* American Society of Civil Engineering.

Baker, J.W. and Cornell, C.A. (2006), "Spectral shape, epsilon, and record selection", *Earthq. Eng. Struct. Dyn.*, **35**(9), 1077-1095.

Benzoni, G. and Priestley M.J.N. (2003), "Seismic response of linked marginal wharf segments", *J. Earthq. Eng.*, **7**(4), 513-539.

Burden, L.I., Rix, G. and Werner, S. (2016), "Development of a risk framework for forecasting earthquake losses in port systems", *Earthq. Spectr.*, **32**(1), 267-284.

California Building Standards Commission (2010), *California Building Code: California Code of Regulations*, Title 24, Part 2, Volume 1, Chapter 31F, Marine Oil Terminal Engineering and Maintenance Standards (MOTEMS).

Chopra, A.K. and Goel, R.K. (2001), "Direct displacement-based design: Use of inelastic vs. elastic design spectra", *Earthq. Spectr.*, **17**(1), 47-64.

Chore, H.S., Ingle, R.K. and Sawant, V.A. (2012), "Non-linear analysis of pile groups subjected to lateral loads using 'p-y' curve", *Interact. Multisc. Mech.*, **5**(1), 57-73.

Computers and Structures (2006), *Inc. PERFORM 3D, User Guide v4, Nonlinear Analysis and Performance Assessment for 3D Structures*.

DesRoches, R., Comerio, M., Eberhard, M., Mooney, W. and Rix, G.J. (2011), "Overview of the 2010 Haiti earthquake", *Earthq. Spectr.*, **27**(S1), S1-S21.

Eberhard, M., Baldridge, S., Marshall, J., Mooney, W. and Rix, G.J. (2010), *The Mw 7.0 Haiti earthquake of Jauary 12, 2010*, USGS/EERI Advance Reconnaissance Team Report.

El-Tawil, S. and Deierlein, G. (2001a), "Nonlinear analysis of mixed steel-concrete frames. I: Element formulation", *J. Struct.*

*Eng*., **127**(6), 647-655.
El-Tawil, S. and Deierlein, G. (2001b), "Nonlinear analysis of mixed steel-concrete frames. II: Implementation and verification", *J. Struct. Eng*., **127**(6), 656-665.
Green, R.A., Olson, S.M., Cox, B.R., Rix, G.J., Rathje, E., Bachhuber, J., French, J., Lasley, S. and Martin, N. (2011), "Geotechnical aspects of failures at Port-au-Prince seaport during the 12 January 2010 Haiti earthquake", *Earthq. Spectr*., **27**(S1), S43-S65.
Kalkan, E. and Chopra, A. (2010), *Practical Guidelines to Select and Scale Earthquake Records for Nonlinear Response History Analysis of Structures*, USGS Open-File Report 2010-1068, Menlo Park, CA, <http://pubs.usgs.gov/of/2010/1068/>.
Kalkan, E. and Chopra, A. (2012), "Evaluation of modal pushover-based scaling of one component of ground motion: Tall buildings", *Earthq. Spectr*., **28**(4), 1469-1493.
Landers, P. (2001), *Kobe Disaster Offers Clues on Rebuilding*, Wall Street Journal, October.
Matlock, H. (1970), "Correlations for design of laterally loaded piles in soft clay", *Proceedings of the Offshore Technology Conference*, Houston, April.
POLA (2012), *The Port of Los Angeles Code for Seismic Design, Upgrade, and Repair of Container Wharves*, Port of Los Angeles.
Port of Seattle (2013), *Foreign Waterborne Trade Report*, Seattle, U.S.A.
Ragued, B., Wotherspoon, L. and Ingham, J. (2014), *Seismic Response of A Typical New Zealand Pile-Supported Wharf Configuration*, New Zealand Society for Earthquake Engineering Technical Conference and AGM, Auckland, March.
Reyes, J.C. and Chopra A.K. (2011a), "Three-dimensional modal pushover analysis of buildings subjected to two components of ground motion, including its evaluation for tall buildings", *Earthq. Eng. Struct. Dyn*., **40**(7), 789-806.
Reyes, J.C. and Chopra, A.K. (2011b), "Evaluation of three-dimensional modal pushover analysis for unsymmetric-plan buildings subjected to two components of ground motion", *Earthq. Eng. Struct. Dyn*., **40**(13), 1475-1494.
Reyes, J.C. and Chopra A.K. (2012), "Modal pushover-based scaling of two components of ground motion records for nonlinear RHA of buildings", *Earthq. Spectr*., **28**(3), 1243-1267.
Reyes, J.C. and Quintero, O. (2013), "Modal pushover-based scaling of earthquake records for nonlinear analysis of single-story unsymmetric-plan buildings", *Earthq. Eng. Struct. Dyn*., **43**(7), 1005-1021.
Reyes, J.C., Riaño, A., Kalkan, E., Quintero, O. and Arango, C. (2014), "Assessment of spectrum matching procedure for nonlinear analysis of symmetric- and asymmetric-plan buildings", *Eng. Struct*., **72**(1), 171-181.
Reyes, J.C., Riaño, A., Kalkan, E. and Arango, C. (2015). "Extending modal pushover-based scaling procedure for nonlinear response history analysis of multi-story unsymmetric-plan buildings", **88**(1), 125-137.
Roth, W. and Dawson, E. (2003), "Analyzing the seismic performance of wharves, part 2: SSI analysis with nonlinear, effective-stress soil models", *Proceedings of the TCLEE 2003: Advancing Mitigation Technologies and Disaster Response for Lifeline Systems*, Long Beach, August.
Saha, R., Dutta, S.C. and Haldar, S. (2015), "Effect of raft and pile stiffness on seismic response of soil-piled raft-structure system", *Struct. Eng. Mech*., **55**(1), 161-189.
Sandoval, J.D. (2015), "Evaluacion del proceso estatico no lineal del estándar ASCE 61-14 para estimar demandas sísmicas en muelles", BSCE Dissertation, Universidad de los Andes, Bogotá.
Shafieezadeh, A., DesRoches, R., Rix, G. and Werner, S. (2012), "Seismic performance of pile-supported wharf structures considering soil-structure interaction in liquefied soil", *Earthq. Spectr*., **28**(2), 729-757.
Shafieezadeh, A., DesRoches, R., Rix, G. and Werner, S. (2013), "Three-dimensional wharf response to far-field and impulsive near-field ground motions in liquefiable soils", *J. Struct. Eng*., **139**(8), 1395-1407.
Shafieezadeh, A. and Burden, L.I.(2014), "Scenario-based resilience assessment framework for critical infrastructure systems: Case study for seismic resilience of seaports", *Reliab. Eng. Syst. Safety*, **132**, 207-219.
Shibata, A. and Sozen, M.A. (1976), "Substitute-structure method for seismic design in R/C", *J. Struct. Eng*., **102**(1), 1-18.
Varun, V., Assimaki, D. and Shafieezadeh, A. (2013), "Soil-pile-structure interaction simulations in liquefiable soils via dynamic macroelements: Formulation and validation", *Soil Dyn. Earthq. Eng*., **47**, 92-107.
Zareian, F., Aguirre, C., Beltran, J.F., Cruz, E., Herrera, R., Leon, R., Millan, A. and Verdugo, A. (2012), "Industrial facilites affected by the 2010 Chile offshore Bio-Bio earthquake", *Earthq. Spectr*., **28**(S1), S513-S532.

*PL*